Studies of water and ice in hydrophilic and hydrophobic mesoporous silicas : Pore characterisation and phase transformations

Jahwar Jelassi [*†] Hessel L. Castricum [‡]

Marie-Claire Bellissent-Funel [*] John Dore [§¶]

J. Beau W. Webber [§‖**] Rachida Sridi-Dorbez [†]

November 25, 2009

Abstract

A study has been made as a function of temperature of the phase transformation of water and ice in two samples of mesoporous silica gel with pore diameters of ∼50 Å. One sample was modified by coating with a layer of trimethylchlorosilane, giving a predominantly hydrophobic internal surface, whereas the unmodified sample has a hydrophilic interface. The pore structure was characterised by nitrogen gas adsorption and NMR cryoporometry and the melting/freezing behaviour of water and ice in the pores was studied by DSC and neutron diffraction for cooling and heating cycles, covering a range of 200 to 300K. Measurements were made for several filling-factors in the range 0.2 to 0.9. The results show a systematic difference in the form of ice created in each of the samples. The non-modified sample gives similar results to previous studies with hydrophilic silicas, exhibiting a defective form of cubic ice superimposed on a more disordered pattern that changes with temperature and has been characterised as 'plastic' ice [Liu et al, 2006, Webber et al, 2007]. The modified sample has similar general features but displays important variability in the ice transformation features, particularly for the case of the low filling-factor (f=0.2). The results exhibit a complex temperature-dependent variation of the crystalline and disordered components that are substantially altered for the different filling-factors.

[*]Lab. Leon Brilloiun, CEA, Saclay, France,

[†]Dept de Physique, Université de Monastir, Tunisie,

[‡]Van't Hoff Institute for Molecular Sciences, Universiteit van Amsterdam, Nieuwe Achtergracht 166, 1018 WV Amsterdam, The Netherlands,

[§]School of Physical Sciences, University of Kent, Canterbury. CT2 7NH,

[¶]J.C.Dore@kent.ac.uk

[‖]Institute of Petroleum Engineering, Heriot Watt University, Edinburgh. EH14 4AS,

[**]Lab-Tools Ltd., Canterbury Enterprise Hub, University of Kent, Canterbury, Kent. CT2 7NJ.

1 Introduction

The characteristics of liquid water, confined in a mesoporous solid, have become a highly topical area of research. Water can be considered as an essential molecule for life and has properties that are unlike those of any other liquid. The confinement of water in small volumes, such as in living cells, changes its structure and dynamics. At lower temperatures, water can be under-cooled and nucleates with the formation of ice structures that are different from the normal form of hexagonal ice-I_h,[1,2]. These effects become especially apparent for confinement in mesoscopic [nm-sized] volumes. Most work has been conducted using solid substrates although there is also interest in water confined in soft matter. Porous silica exists with various well-defined pore sizes, which allows the variation of the geometrical parameters in a controlled and straightforward manner. The solid substrate also enables the water/ice properties to be studied for complete and fractional-pore-filling, using a range of experimental and simulation techniques[3,4,5,6,7].

The silica surface is essentially hydrophilic in character due to the presence of silanol groups[8] and consequently there is a specific interaction at the interface that influences the behaviour of the water volume in the pore. The modification of the characteristics will depend on the proximity and the length scale for the effects is not yet well defined. As a result, the properties of the confined water phase are found to be dependent not only on the pore size, pore morphology and the fractional-filling but also on the surface density of Si-OH (silanol) groups. It is therefore of interest to modify the surface characteristics and to investigate the properties for water at a more hydrophobic or non-polar interface. The surface silanol density can be reduced by a heat treatment at elevated temperatures, leading to silanol condensation and the formation of Si-O-Si. However, this process is reversible upon re-exposure to water and may also lead to an irreversible and substantial change in porosity[8]. A more convenient way of changing the interfacial features without essentially changing the pore size and morphology is by grafting a layer of co-valently-bonded functional groups onto the bare silica surface. This procedure involves chemical treatment of the silica sample, which, in the current experiments, has utilised trimethylchlorosilane to give a hydrophobic 'methylated' surface. This procedure has been found to be suitable for the samples investigated in this study, giving the least change in pore size[9]. In this first paper we describe the structure of both the non-modified and modified (methylated) silica and the formation of ice upon cooling of confined water in the two different silica materials by using a combination of several techniques. Ice formation in the two materials has been studied for various filling factors. Complementary measurements on the 'non-modified' and 'modified' materials, including N_2 vapour adsorption (GA), differential scanning calorimetry (DSC), NMR cryoporometry (NMR-C) and neutron diffraction (ND), have also been conducted.

2 Experimental techniques

2.1 Materials preparation

Mesoporous silica gels are available commercially and have an inter-connected disordered network. Silica gel (35–70 μm grain diameter, >99.5% SiO_2, Grace Davison SI 1404) with a mean pore diameter in the range 50-70 Å, was heated in air at 773 K for 5 hrs to remove any adsorbed species and to obtain a moderate degree of hydroxylation. This 'non-modified' material was hydrophobised by dropwise addition of 5.25 ml trimethylchlorosilane ($(CH_3)_3SiCl$, TMCS, 99% pure, Aldrich) to 8.67 g of silica in a mixture of 50 ml water (doubly-distilled) and 21.6 ml of isopropanol (Aldrich, 99.9% pure), and subsequent refluxed for 30 min during continuous stirring. Prior to the TMCS addition, the material was left in the liquid mixture for 5 min. After modification, the materials were dried, washed three times with water/ethanol and dried in air at 393 K[9]. The untreated silica provides the hydrophilic sample, classed as 'non-modified', and the treated sample with a predominantly hydrophobic interface provides the 'modified' sample material with a methylated surface.

2.2 Materials Characterisation: Gas adsorption measurements

Adsorption/desorption isotherms of N_2 (77 K) were determined on a CE-Instruments Sorptomatic 1990. All materials were pre-treated by evacuation below 10^{-7} bar at 473 K. Continuous corrections were made for variations in the atmospheric pressure p_0. The results for both samples are shown in Figure 1a for nitrogen. Surface areas and C-values were determined by BET-3 fits from the N_2 adsorption isotherms[10,11] between p/p_0=0 and 0.5, according to:

$$n/n_m = \frac{C(p/p_0)}{(1-p/p_0)} \cdot \frac{1-(N+1)(p/p_0)^N + N(p/p_0)^{N+1}}{1+(C-1)(p/p_0) - C(p/p_0)^{N+1}}, \qquad (1)$$

where n in the gas adsorbed at relative pressure p/p_0, n_m is the monolayer capacity of the surface, [units mol.g$^-$1], C a constant related to heat of adsorption (and thus dependent on the adsorbate-adsorbent interaction) and N the number of adsorbed layers. The area occupied by a N_2 molecule in the completed monolayer was taken to be 0.162 nm^2 (ISO 9277)[12]. Mesopore size distributions and mean mesopore diameters were obtained from BJH fits of the desorption isotherms[13] between p/p_0=0.35 and 0.9, assuming cylindrical pores. A zero contact angle was assumed between the silica surface and nitrogen liquid in the Kelvin equation used in BJH analysis. Values for the thickness of the t-layer (the film thickness t, due to multilayer adsorption) were used with a dependency on the interaction between adsorbate and adsorbent (i.e. on C), as determined by Lecloux[14]. The total mean pore diameters, (including micropores and assuming cylindrical pore shape) were obtained from the relation[11]:

$$d_p = \frac{4v_p}{A}, \qquad (2)$$

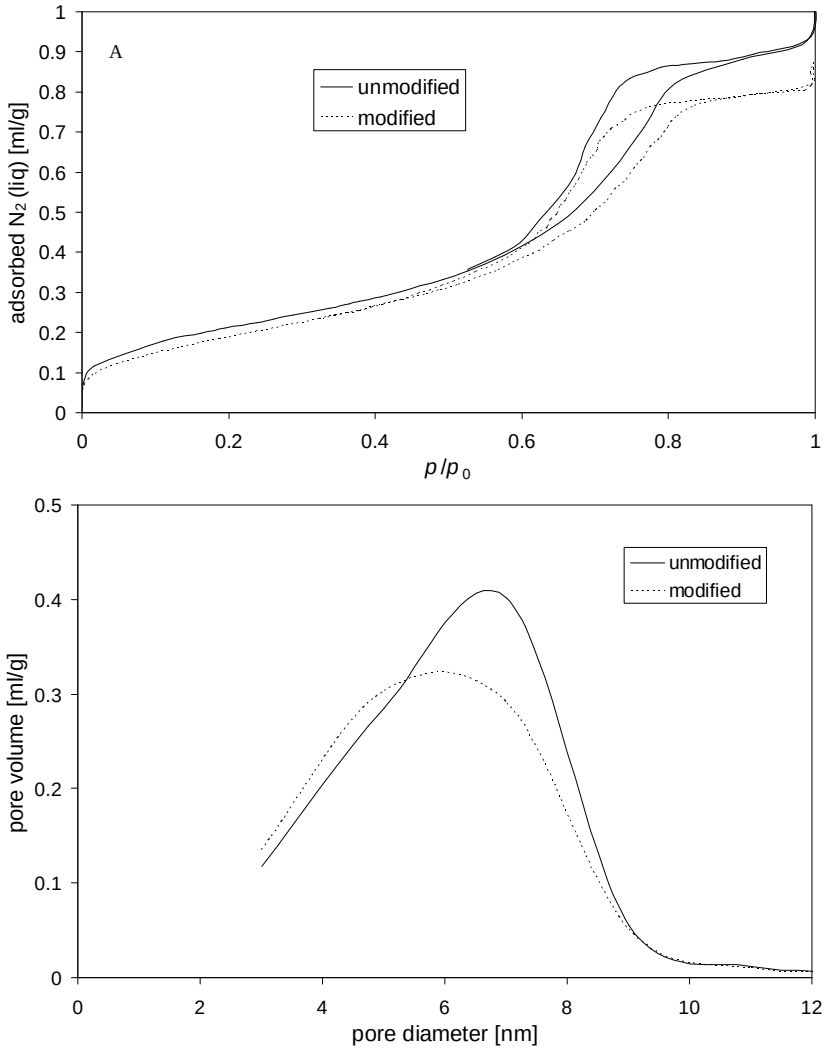

Figure 1: a) Nitrogen adsorption/desorption for non-modified and modified mesoporous silica samples. b) Corresponding pore diameters.

where d_p is the pore diameter, v_p is the pore volume determined at p/p_0=0.95 and A is the surface area. In order to compare the pore volumes of the different samples, the isotherms are displayed in terms of volume of adsorbed nitrogen liquid, assuming a density of 0.8086 g/cm^3 for N_2. The Kelvin equation is used to calulate pore diameter distributions (Figure 1b), and as expected the modified sample shows a smaller remaining free volume.

2.3 Materials Characterisation: Differential Scanning Calorimetry

Differential scanning calorimetry (DSC) has become a standard method for investigating the thermal features of confined fluids. There is a depression of melting point, for the confined fluid, which follows the Gibbs-Thomson relation, which may be written[15] as:

$$\Delta T_m = \frac{k_{GT}}{x}, \tag{3}$$

where k_{GT} is a calibration constant that relates to the thermodynamic variables and x is a length/dimension that depends on the pore size. In the present case, the samples are fabricated by the sol-gel route and the pore network is therefore disordered, although a narrow distribution of effective pore sizes is expected as discussed further in Section 3.3.

DSC measurements were made for the three hydration levels of heavy water, D_2O, corresponding to filling factors of f = 0.95, 0.45 and 0.20 (determined gravimetrically), over a temperature range of 293-135 K in cooling and heating mode; the results are shown in Figure 2. In each case the behaviour of the modified and non-modified samples shows significant variations and there is a large change for the different hydration levels.

For f = 0.90, an initial measurement with a ramp rate of 10K/min revealed a broad exothermic peak in the region of 243K and a second measurement was made with a rate of 2K/min to improve the resolution. The results for the slower rate (for both cooling and heating) are shown in Figure 2a, with an inset for the transition region. The onset of the energy flow is seen to occur at a higher temperature for the modified sample. The unusual shape is indicative of a two-step process and will later be shown (Section 3) to arise from a separate nucleation and growth process. The heating curve reveals a broad endothermic peak that extends over 30K and corresponds to the melting of the ice in the pores. These results indicate a hysteresis effect due to non-equilibrium supercooling of the liquid in the pores, but it is notable that the base line is not flat and that energy flow is occurring over a large temperature range.

The data for the f=0.45 case were taken for a ramp rate of 10K/min and give a single asymmetric profile that represents a phase transition at 241K with an indication of precursor changes at higher temperatures. The main peak position is displaced to slightly lower temperatures relative to that for the f=0.9 case but this may be a consequence of the faster scan rate. Nevertheless, there seems to be a much smaller contribution in the pre-transition region. The heating cycle has a similar shape for the endothermic change but it is notable that the

difference in magnitude of the peaks for the different samples is increased for this case.

The f=0.20 case shows two distinct exothermic events. The first peak occurs at a similar temperature to the main peaks for the other cases but the second peak is displaced to lower values for the modified silica relative to the unmodified silica. The origin of this double-transition region is still unclear as it does not correspond to an obvious transition in the ice structure but can be linked to the distribution of partially-filled pores. The endothermic peaks also show considerable variation. They are very broad and the peak for the modified silica again occurs at a lower temperature, the difference in the endothermic peak between the two samples is larger (7K) for this case. It is also clear that the background levels are not flat for any of the samples. The complete set of transition temperatures for D_2O is listed in Table 1a and the results are compared with the data for H_2O from the NMRC measurements in Section 2.4 (Table 1b).

a)

D_2O Filling factor	f=0.9		f=0.45		f=0.2	
DSC Samples	non-mod	mod	non-mod	mod	non-mod	mod
exothermic pk 1 (K)	243	243	241	241	242	242
exothermic pk 2 (K)	244	245			235	233
endothermic pk (K)	267	267	268	266	264	257

b)

H_2O Filling factor	f=1.98	f=1.69	f=0.63
NMR Samples	non-mod	mod	mod
warming (K)	262.6	262.0	262.8

Table 1: The temperatures of phase-transitions in the DSC and NMR measurements.
a) The temperatures of different peaks in the D_2O DSC measurements for cooling and heating cycles. Values are given for the two peaks shown in Figures 2a and 2c.
b) The melting temperatures for the different H_2O NMR cryoporometry measurements.

2.4 Materials characterisation: NMR cryoporometry

Nuclear magnetic resonance cryoporometry[15,16] is a convenient way of determining pore size through an alternative application of the Gibbs-Thomson relation (eqn. 3). A comparison of different techniques for determining porosity suggests that the k_{GT} calibration constant is, as theoretically expected, dependent on pore geometry, but a full understanding of these factors is still being developed[7,17,18,19,20].

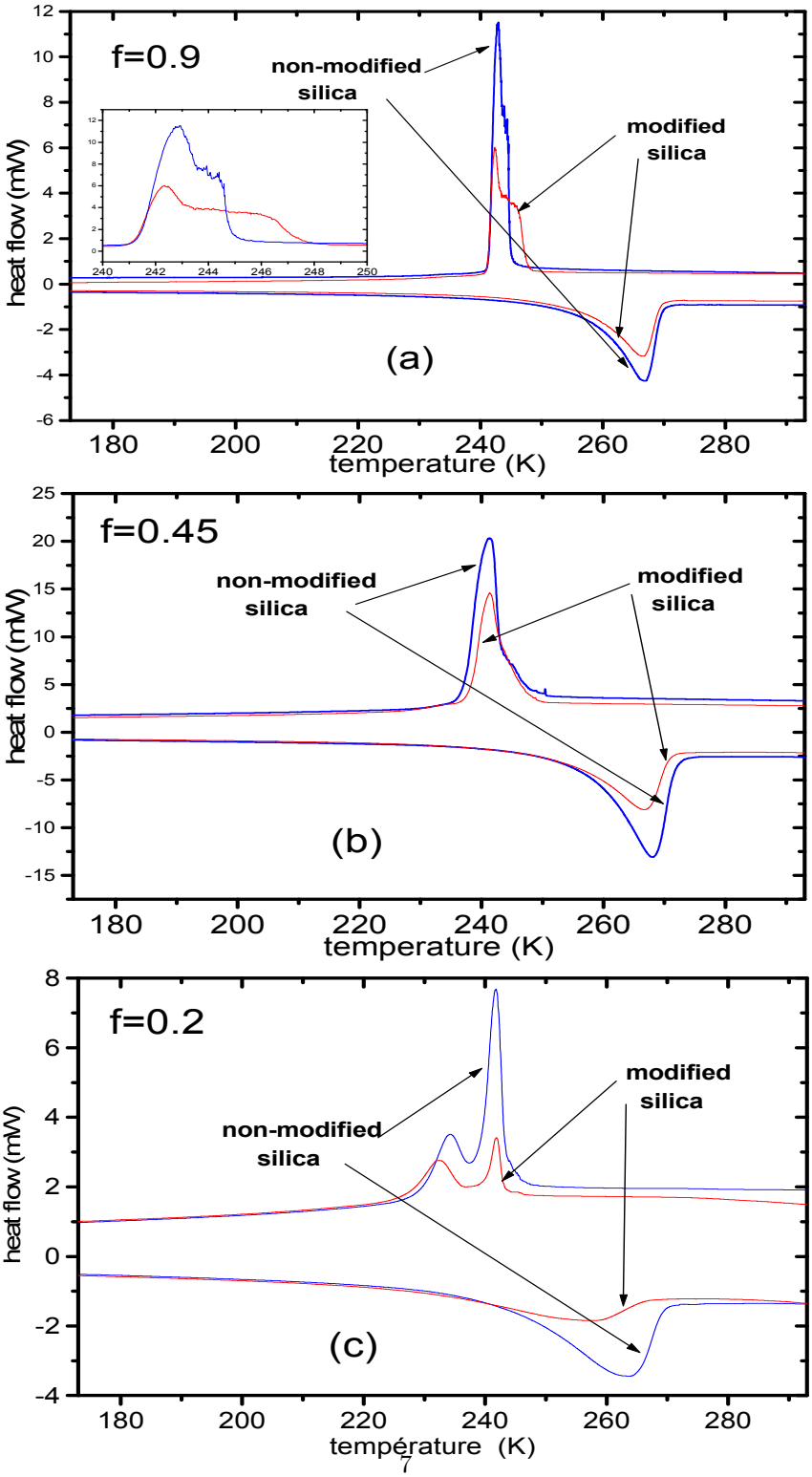

Figure 2: DSC measurements for D_2O water in the non-modified and modified samples with filling factors, f, of a) 0.90, b) 0.45 and c) 0.20. The upper traces are for cooling, the lower traces are for warming.

Measurements were made for the modified and non-modified materials using over-filled and partially-filled samples. The amplitude of the NMR signal at time (2τ= 2ms), which defines the quantity of H_2O in the liquid state, was monitored as a function of temperature for cooling and heating cycles in each case, using temperature scanning rates of 0.1 K.min^{-1}; the results are shown in Figure 3. These data give the pore volumes as 0.684 ml.g^{-1} (unmodified) and 0.598 ml.g^{-1} (modified). However a correction needs to be made for the faster relaxation time of the liquid in the pore compared with that of the bulk liquid; the values from both techniques are given in Table 2.

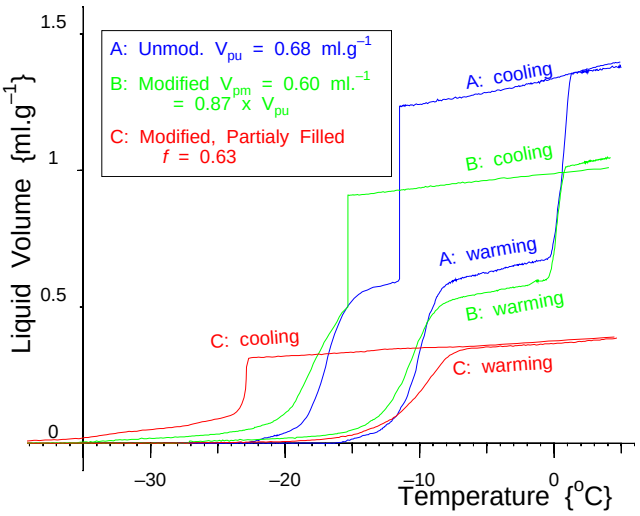

Figure 3: NMR cryoporometry measurements for H_2O water in a non-modified sample with filling factor f=1.98, showing pore volume (unmodified) V_{pu} = 68 ml.g^{-1}; a modified sample with f=1.69, showing pore volume (modified) V_{pm} = 60 ml.g^{-1}; and for a modified partially-filled sample with a filling factor f=0.63; for both cooling and warming ramps.

Using a k_{GT} value of 582 K.Å appropriate to sol-gel silicas, the data can be converted to a pore size distribution function[21] and the results are shown in Figure 4 and Table 2. The cryoporometry results appear to be more fully resolving the pore size distributions, and a narrower size-distribution is obtained than that from the gas adsorption measurements Figure 1b. A comparison of the pore size and pore volume characteristics determined from the different experimental techniques is presented in Section 4.1.

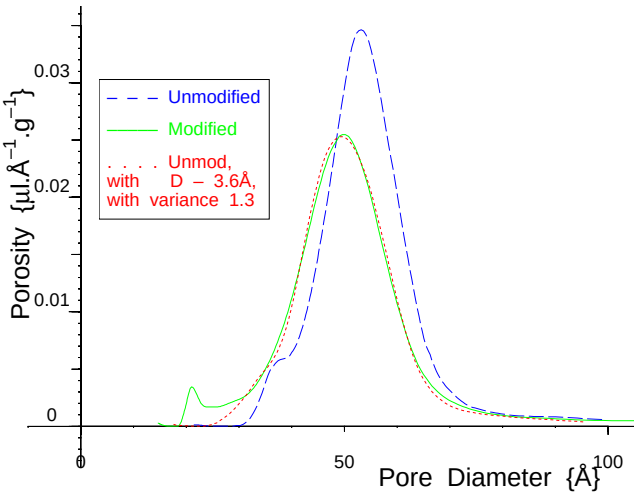

Figure 4: The pore size distribution function for both modified and unmodified samples, determined from the NMRC data of Figure 3. Also plotted is the calculated distribution due to a surface layer with thickness 1.8 Å, with a variance of 1.3.

Silica gel	v_p cm^3/g	$A(N_2)$ m^2/g	Mean d nm	BJH d nm	v_p cm^3/g	$d_p{}^{sol-gel}$ nm
	N_2 adsorption				**NMRC**	
non-mod	0.840	472	7.12	6.09	0.694	5.31
Mod	0.755	438	6.90	5.96	0.608	4.99

Table 2: Pore characterisation by N_2 gas adsorption and NMR Cryoporometry.

3 Neutron diffraction measurements for confined water and ice

3.1 Experimental procedure

The structural characteristics of the water in the pores can be conveniently studied by neutron diffraction. The measurements were made on the 7C2 diffractometer at the Orphée reactor, Lab. Leon Brillouin (LLB), Saclay[22]. Several different levels of hydration with D_2O were used for both the modified and non-modified silica samples. The scattered intensity was measured for a 0.7 Å incident beam at several fixed temperatures covering a Q-range of 0.1 - 16 $Å^{-1}$. The data were recorded for the normal liquid phase, the under-cooled liquid phase and the crystalline/disordered ice phases, covering a temperature range of 215 to 295 K in both cooling and heating cycles. The temperature ranges for the runs are listed in Table 3, the actual measurements being made at well equilibrated spot temperatures. The scattering intensities are shown (as a function of Q) in Figure 5 for the 'wet' and 'dry' samples at two different temperatures and also for the cryostat background. The profile for the confined water/ice can be obtained by subtracting the measurement for the 'dry' silica from the measurement for the 'wet' silica. This method does not eliminate the water-silica cross-terms arising from correlations across the interface but still gives valuable information about the general structure of the water or ice formed in the pores. The use of a temperature difference technique provides a route to the observation of structural variations as a function of temperature and is less influenced by systematic errors.

Filling factor	f=0.9		f=0.45		f=0.2	
Sample	non-mod	mod	non mod	mod	non- mod	mod
Liquid/cooling	297-273	297-275	297-260	297-255	297-255	297-255
Solid/ cooling	268-210	268-220	245-200	249-220	240-200	240- 220
Solid / heating	238-268	238-268	245-260		255	

Table 3: Temperature ranges (K) for the neutron measurements.

3.2 Non-modified silica

The diffraction profiles for the liquid and ice phases in the non-modified sample are shown for an intermediate Q-range in Figures 6a and 6b and the cooling and heating cycles for f=0.9 . The pattern for Q>6 $Å^{-1}$ is identical for all temperatures and has a shape that corresponds closely to the molecular form-factor for D_2O, although there are some deviations that will be discussed in Section 4. In the cooling run (Figure 6a) there is a continuous evolution of the peak intensities after the initial nucleation. The corresponding data for the heating run are given in Figure 6b and show reversible behaviour with the

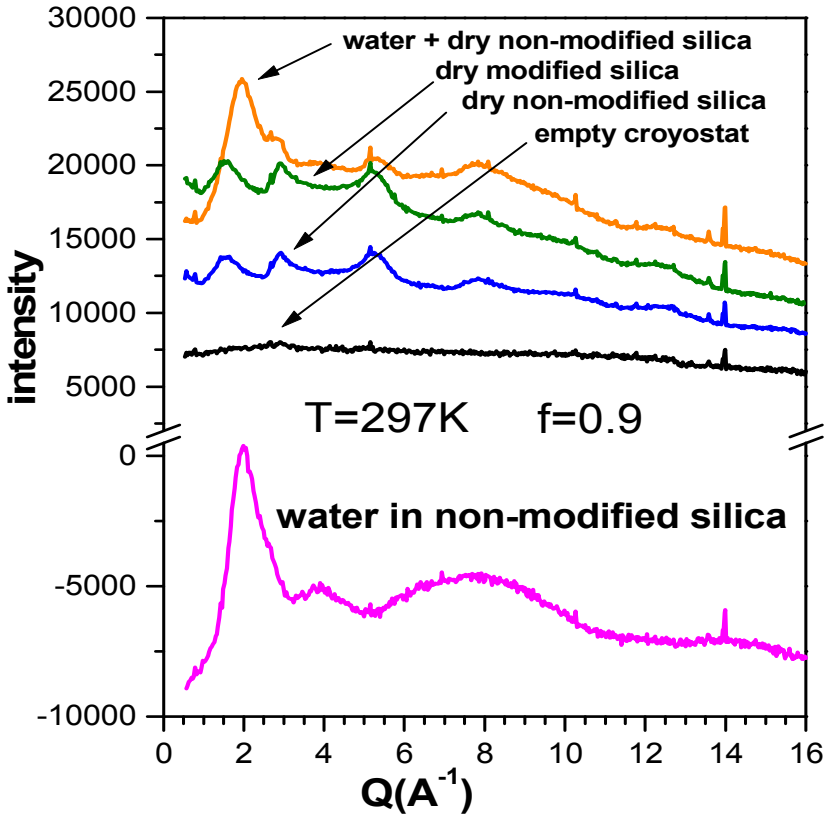

Figure 5: The measured intensity profiles for neutron scattering from 'dry' and 'wet' silica samples with the cryostat background; the pattern for the water is shown below

.

melting of the ice occurring at a higher temperature and therefore confirming the hysteresis effect seen in the DSC data.

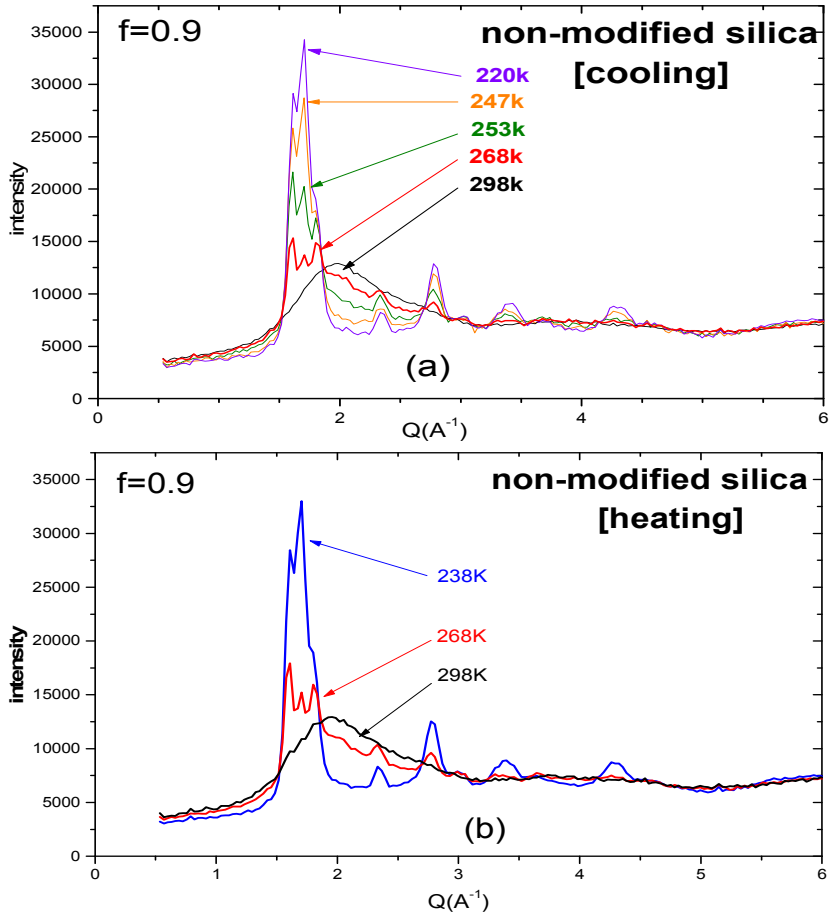

Figure 6: The superimposed diffraction patterns for water/ice in the non-modified silica sample as a function of temperature; showing the low-Q region on an expanded scale: a) cooling sequence, b) heating sequence.

The onset of nucleation appears to be in the region slightly above 268K corresponding to a Gibbs-Thomson depression of ∼10 K (for D_2O). The diffraction pattern at this temperature shows the characteristic triplet (1.5-2.0 Å^{-1}) of hexagonal ice [I_h] superimposed on a diffuse distribution that is similar to the liquid phase at a higher temperature. As the temperature is further reduced, the intensity of the central Bragg peak increases continuously down to 215K, indicating the predominant growth of a cubic ice [I_c] phase. It is also interesting to note that the next peak above this main peak, at 2.36 Å^{-1}, which can be assigned solely to ice-I_h, grows initially between 268 and 260K. The intensity

does not change at lower temperatures, whereas the other peaks at 2.82, 3.40 and 4.29 $Å^{-1}$ all follow the intensity variation of the central triplet peak. These results suggest a two-stage process in which the initial nucleation event causes a fraction of the water to crystallise as hexagonal ice but the subsequent growth is predominantly in the form of cubic ice. This feature is similar to that observed in the detailed studies of ice nucleation in SBA-15 silica samples with a pore size of 86 Å [23,24,25] and is discussed more fully in Section 4.

It is also clear from the region between the peaks that there is always a significant diffuse scattering component. The region 1.9 to 2.9 $Å^{-1}$ shows a continuous reduction in intensity over the whole temperature range and represents the sequential conversion of a disordered phase to a crystalline one as the temperature is reduced. However, the intensity between the Bragg peaks never falls to zero and is therefore indicative of a remaining disordered phase, even at the lowest temperatures. It is impossible to determine from the diffraction data whether this component is in the form of a deeply-supercooled liquid or has formed a glassy state in which the molecular diffusion has become severely restricted. Other studies by NMR on mesoporous silicas suggest that the relaxation processes are intermediate between the normal liquid and brittle ice such that the term 'plastic ice' has been used to describe this intermediate state [7,26].

The results for the heating cycle are shown in Figure 6b. The changes in the shape of the diffraction pattern are completely reversible, indicating a reduction of the cubic ice component up to 268 K and the re-emergence of the hexagonal ice triplet peak superimposed on the diffuse scattering component. This feature is surprising as it corresponds to an apparent metastable behaviour in which the proportion of crystalline and disordered material is inter-convertible and is dependent on the absolute temperature and not on the thermal history. The ice eventually melts at a higher temperature to produce liquid water and displays a hysteresis effect as observed in the NMR cryoporimetry data. Another characteristic of the diffraction data, shown in Figure 6 is the behaviour at low-Q values. This region is shown on an expanded scale in Figure 7 and discussed in Section 3.4.

3.3 Modified silica

Similar measurements have been made for the modified sample. The basic features of initial nucleation as hexagonal ice at 269 K are reproduced and also the subsequent growth as cubic ice below 258 K. In this case, the hexagonal ice component appears to be much smaller than in the case of the non-modified silica, such that the final profile at 220 K shows a predominant central peak for ice–I_c. However, the heating cycle again shows the disappearance of the cubic ice to leave an ice-I_h profile at 268 K. The fact that water is readily adsorbed into the modified silica with its hydrophobic interface suggests that complete coverage of the internal surfaces does not occur and that the adsorption process involves an initial formation of water droplets at specific sites in the pore volume. As a result, there will be some water that is in proximity to hydrophilic regions and will behave in a similar way to the non-modified sample.

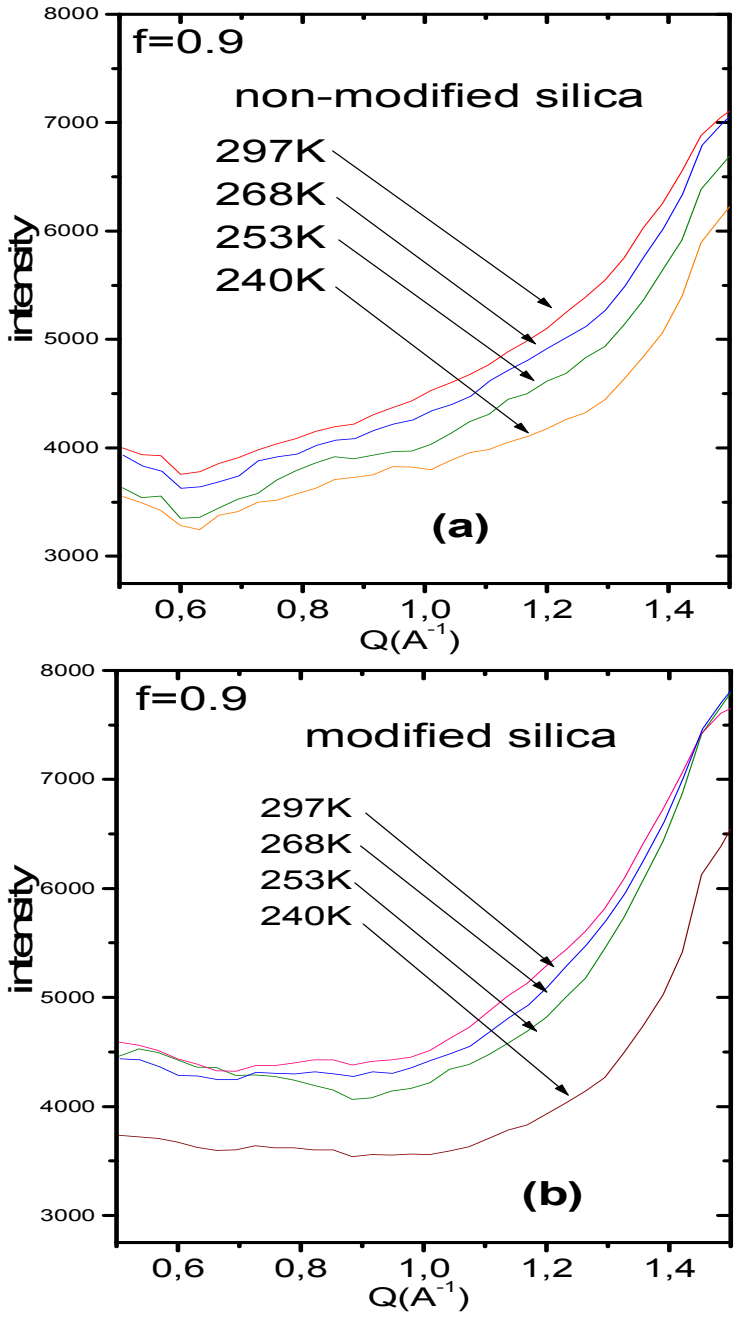

Figure 7: The change in the low-Q intensities as a function of temperature a) non-modified silica, b) modified silica.

Consequently it would seem from the difference in the ice patterns that the hydrophobic surface promotes the growth of cubic ice rather than hexagonal ice. However, the temperature-dependent characteristics appear to be very similar for both modified and non-modified samples. The low-Q behaviour also has a similar temperature dependence. A more detailed consideration of the structural changes by temperature-difference analysis is deferred until Section 4.2.

3.4 Scattering patterns at low Q-values

The asymptotic value of the structure factor, S(Q), as Q approaches zero, is related to the isothermal compressibility, χ_T. All the datasets show a systematic change of intensity with temperature in the range 0.5-1.5 $Å^{-1}$ that is indicative of a continuous but gradual reduction of the measured intensity as the temperature is reduced. However, the behaviour at lower Q-values cannot be observed due to the strong SANS signal caused by the small-angle scattering contribution from the mesopore structure. The liquid phase is more compressible than the solid and therefore gives a higher value for the intercept. However, there is no evidence for a sharp change in the level that could be taken as an indication of an abrupt change of state from the liquid to the solid. Although the meaning of $\chi_T$in these circumstances may be open to interpretation and the accessible region is not close to Q=0, it seems that the transformation of the liquid to a plastic-ice state exhibits a gradual change as a function of temperature. There is a difference in shape between the non-modified and modified samples, as revealed in Figure 7, but the higher value could be due to the presence of the thin hydrophobic layer that alters the contrast profile. Further studies using a dedicated SANS instrument are clearly needed.

4 Analysis and interpretation

4.1 Comparison of sample characteristics

Three different techniques have been used to characterise the pore size, namely gas adsorption, DSC and NMRC. The parameters obtained from the experimental measurements are summarised in Tables 1 and 2. The DSC and NMRC methods both rely on the use of the Gibbs-Thomson relationship and should therefore be closely linked although one measurement uses D_2O and the other uses H_2O. The equivalent thermophysical quantities show a positive isotopic shift of typically 4-6 K from H_2O to D_2O, so that the figures given in Table 1 are consistent. There is a fundamental question relating to the value of the constant, k_{GT}, in the Gibbs-Thomson equation, (eqn 1), with regard to the geometry of the pore[7,19]. These considerations are too complex to present here and the results quoted in table 2 are based on the assumption of sol-gel-like pore-morphology, for which a value of 582 K.Å for $k_{GT}$is appropriate[21].

An important discrepancy is apparent between the results for the pore diameters for the unmodified and modified silicas, for gas adsorption (Mean 71.2

and 69.0 Å), (BJH 60.9 and 59.6 Å) and for NMR cryoporometry (53.1 and 49.9Å). Even if there is some uncertainty in the k_{GT} value, this discrepancy is well outside experimental error and requires some further explanation. The two most likely reasons are that a) the geometries of the liquid/vapour interface is different from that of the solid/liquid interface, and b) that the nitrogen gas can enter parts of the pore volume that are not accessible to water molecules. A similar difference has been noted in studies of SBA-15 silicas[7,19,20] and appears to relate to the incomplete filling of the micropores with water. It is, of course, impossible to say how the distribution of nitrogen and water in the pores may differ, as the adsorption is dependent not only on the pore dimensions but also on the molecular size and the interaction with the surface. The NMRC studies are made with an over-filled sample and the extracted quantities of intra-pore and inter-pore water are determined on an absolute scale. However, it is also notable that an NMRC measurement made at a single echo time will tend to under-estimate the correct pore volume due to the T_2 relaxation in the pores being faster than that of bulk liquid; a compensation has been made for this effect but further work is necessary. At this level of accuracy, the comparisons are considerably more complex than can be indicated here.

The calculation of the correct filling-factors relies on the evaluation of the absolute pore volume available to the water. The uncertainties described in the previous paragraph suggest that the true volume is greater than that obtained from the NMRC data but less than that obtained from the nitrogen gas adsorption data. At the time of the experiment only the gas adsorption data were available and an allowance was made for change in volume due to the thickness of the hydrophobic layer. Under these conditions, the filling factors were chosen to be i) 0.90 ± 0.01 and ii) 0.45 ± 0.01 for each of the samples and for the lower filling factors, the values were iii) 0.17 and 0.22 ± 0.02 for the non-modified and modified samples respectively. Although the absolute values are subject to uncertainties, the relative values for the fractional-fillings remain fixed. The f-values listed on the graphs correspond to these values and may be a slight under-estimate of the true values. The small differences are not expected to materially affect the conclusions of the overall investigation and the differences may subsequently be explained in terms of the variation of the k_{GT} value with pore shape, which is not well-defined for sol-gel silicas. Within the uncertainties detailed above, it is pleasing to note that both gas adsorption and NMRC methods give a reasonably consistent value for the difference between the two samples and yield a value of 1.1 ± 0.5 Å for the mean thickness of the deposited hydrophobic layer.

4.2 Phase transformation and ice formation

The neutron data described in Sections 3.2, 3.3 indicate a two-stage process in the formation of ice for the f=0.9 hydration level. These features can be more directly observed by using the temperature-difference function. Figure 8a shows the change in the diffraction pattern for the temperature range 297K to 260K for both samples. The hexagonal ice component appears to be much

smaller than in the case of the non-modified silica. The hexagonal ice pattern is formed by a reduction in the broad diffuse pattern of the liquid phase. In contrast, the difference function between 220K and 260K shown in Figure 8b indicates the growth of cubic ice with a single peak at 1.7 $\AA^{-1}$ for the lower temperature region, but with a much bigger component for the modified silica than in the case of the non-modified silica. There is also a reduction of the diffuse component even at the low temperatures

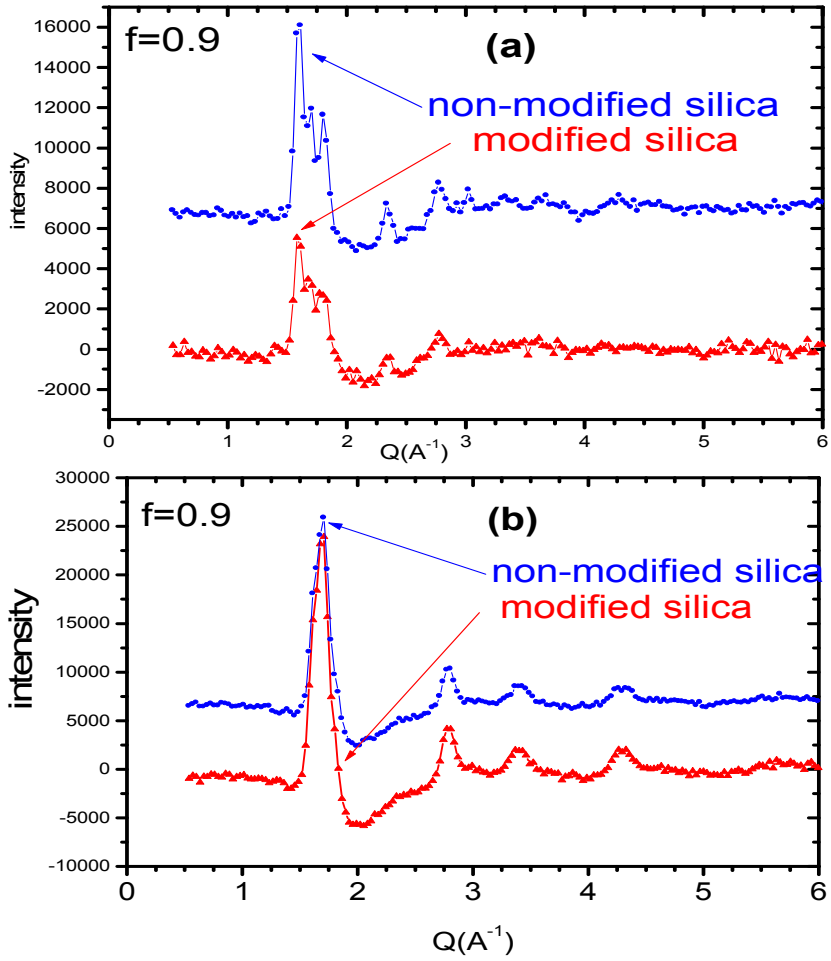

Figure 8: The growth of ice for f=0.9, shown as a difference function for both samples a) between 297 and 260K, and b) between 260 and 220K.

For the f=0.45 case, there is no evidence for the formation of hexagonal ice and the temperature difference function provides evidence for cubic ice formation over the whole temperature range. For the 0.2 hydration level, there is substantial diffraction broadening so that distinct ice peaks are not observed

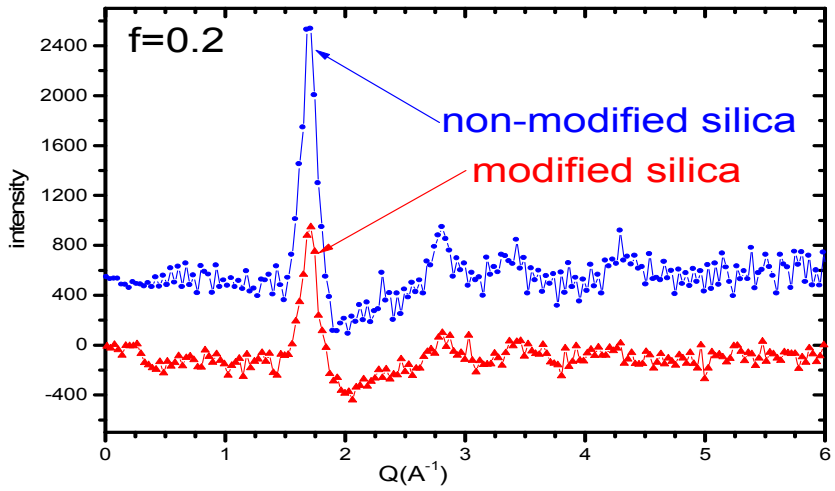

Figure 9: The growth of ice for f=0.2, shown as a difference function for both samples between 255 and 220K.

but the difference function still shows a conversion from the disordered phase to a more ordered phase as indicated in Figure 9. The different features arising from variable hydration allow some additional conclusions to be drawn:-

4.2.1 f=0.90

The hexagonal ice is presumably formed at the centre of the almost fully-filled pores[23]. As the temperature is reduced the liquid/glass phase around the central crystallite converts to cubic ice in both samples, leaving a liquid-like layer at the interface which does not crystallise. In effect the central core of ice expands radially as the temperature is reduced and it is not sensitive to the nature of the interface.

4.2.2 f=0.45

At lower temperatures (∼220K) it is unlikely that the molecules are mobile so this component is expected to be in the form of an amorphous or brittle ice phase. Figure 10 shows the data for the non-modified sample at 200K and 220K with the difference function shown below. It is clear that there is no change in the structural features and therefore any residual motion of the water molecules has been suppressed. This is consistent with the NMR relaxation results, where the relaxation times of the interfacial layer tend towards that of the brittle crystal[7,26].

The diffraction patterns for the f=0.45 case are shown in Figure 11a and 11b for several temperatures. At temperatures of <245K there is evidence of a single main peak corresponding to cubic ice for both samples. These features

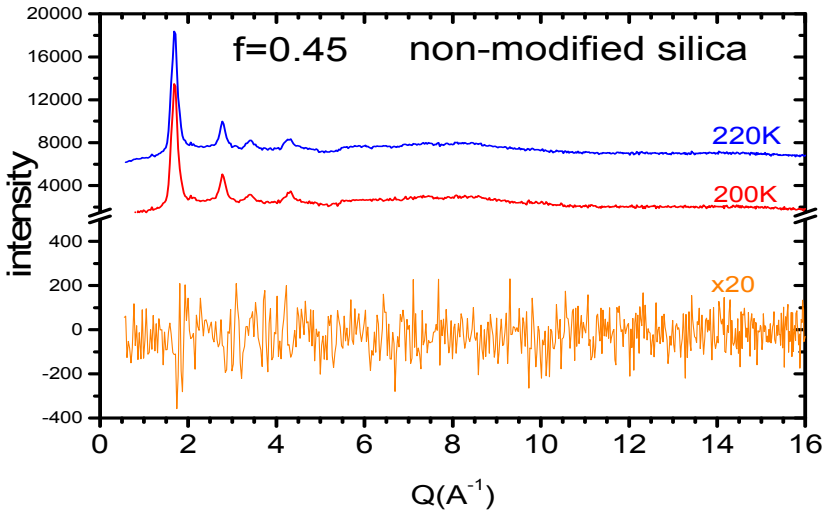

Figure 10: The diffraction pattern for the non-modified sample with f=0.45, between 220 and 200K; the difference function is shown below.

are in agreement with the DSC data that show a single transition with a peak at 241K although there is an indication of some pre-cursor conversion at slightly higher temperatures that probably reflects the distribution of pore sizes. There are changes in the height of the peak as the temperature is further reduced to 220K and it seems that the crystalline component forms more readily in the non-modified sample. This difference is apparent from the comparison of the heights of the main Bragg peak and the reduction in the levels of the diffuse scattering component in the 2.0 to 2.5 Å^{-1} region. Three additional peaks occur at larger Q-values but they are of much lower intensity and appear to be sitting on top of a broad distribution that closely corresponds to the molecular form-factor for the isolated D_2O molecule. The neutron results therefore indicate a single phase transition with the formation of cubic ice from super-cooled water, although it is spread over a wide temperature range.

4.2.3 f=0.20

The temperature variation data for the f=0.2 case show an unexpected change in the overall scattering intensity that is systematic across the whole temperature range and seems to correspond to a constant level (i.e. independent of Q). However, the puzzling feature is that the variation with T is in the opposite direction for the two samples. The results are shown in Figure 12a and b, and in more detail for the low-Q region (<6 Å) in Figure 13a and b. The reduction in temperature gives an increase in the overall level for the non-modified silica and a decrease in the level for the modified silica. The possibility of loss of water from the sample volume illuminated by the incident beam can be ruled

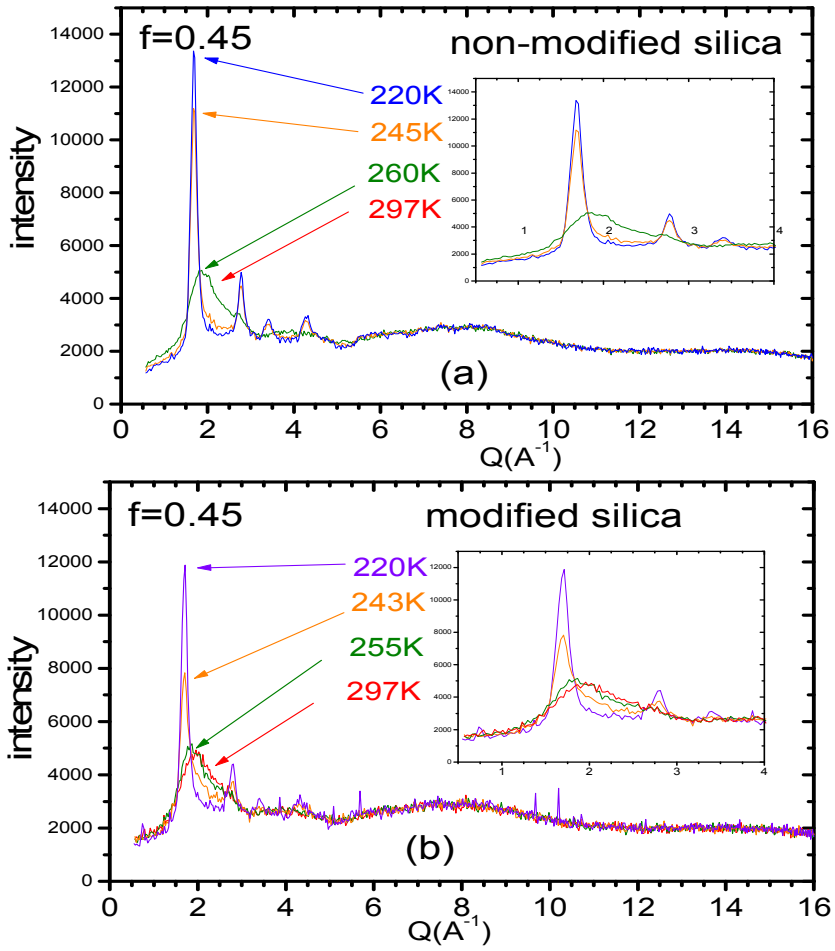

Figure 11: The diffraction patterns for f=0.45 for both samples at several temperatures.

out as this would lead to a change in the high-Q diffraction profile that would be related to the molecular form-factor and easily seen in the difference function. Therefore, the only possible explanation for this effect rests with the inelasticity effects in the scattering process. As the interference terms do not seem to be affected, the temperature-dependent behaviour must arise from the spin-incoherent and coherent self-terms in the cross-section and refers primarily to the dynamic characteristics of the deuterium nuclei.

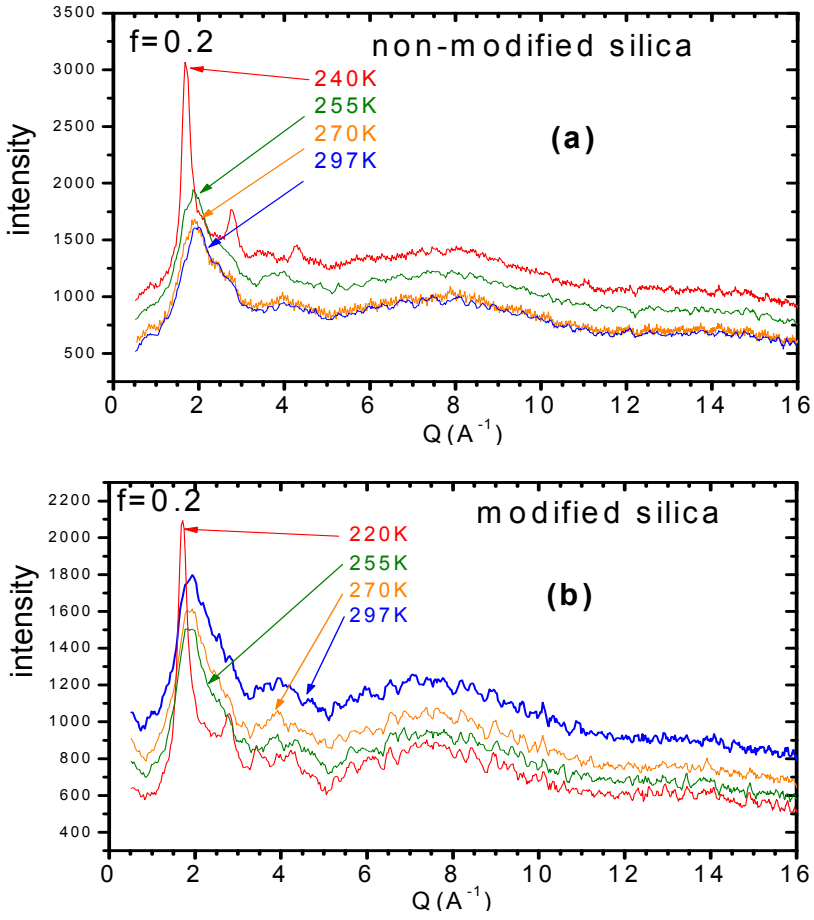

Figure 12: The diffraction patterns for f=0.2 at various temperatures for a) non-modified and b) modified samples.

The inelastic corrections to structure factor measurements were originally discussed by Placzek[27] for monatomic liquids and subsequently adapted to molecular liquids by Powles[28]. The case of D_2O has received particular attention[29]. A full expression for the scattering cross-section requires the inclusion of

an effective recoil mass for the scattering centres so that the observed variations imply that there is a significant change in the effective recoil of the deuterons. The cross-section is higher for the limiting condition of the 'bound atom' case and lower for the 'free atom' case. The results therefore suggest that the reduction in temperature leads to the deuterons becoming 'less bound' in the case of the non-modified silica and 'more bound' in the case of the modified silica. At first sight it would seem likely that the interfacial water for both samples would become more 'bound' as the temperature is reduced due to the loss of thermal excitations and a reduction of both rotational and translational motion. However, there will also be a difference in the hydrogen bond connectivity and a related change in the density profile close to the interface so that the behaviour is not predictable on a simple basis. As most of the molecules are close to the interface, this result indicates that the differences that may relate to changes in the local hydrogen bonding or a possible variation in the density profile close to the interface that influences the dynamics. In the case of the non-modified silica, the first layer of water molecules will be primarily bonded to siloxyl groups, whereas, in the case of the modified silica, the water molecules will be oriented to make hydrogen-bonds within the water/ice layer. There is clearly a need to investigate this effect further by direct spectroscopic measurements, either by quasi-elastic neutron scattering or nuclear magnetic resonance.

Some studies have been reported for under-cooled water in Vycor[30] and related work at protein interfaces[31] suggests that it is the rotational motion that is responsible for this variation, which is consistent with the formation of plastic ice[26]. Figure 13a and b also show some variations in the diffraction profiles between the two samples. The Bragg peak at 1.7 Å^{-1} is slightly more intense for the non-modified silica showing that there may be a larger proportion of ice for this case at 220K. At 240K, this peak is already developed for the non-modified silica but still shows a broad asymmetric peak of lower intensity for the modified-silica sample. Both of these changes occur in a temperature region that is just below the main peak of the DSC data [Figure 2] and above the temperatures of the secondary peak where there is also a displacement to lower values for the modified sample relative to that of the non-modified sample.

A close examination of the shape of the low-temperature curves in the region beyond the main peak suggests that there is a broad peak at 2.8 Å^{-1} and a small dip at 3.2 Å^{-1}. Although the accuracy is limited by the statistics, this effect seems consistent for several datasets and is clearly different for the behaviour of the water/ice in the f=0.45 case. This shape is reminiscent of the diffraction pattern for low-density amorphous [lda] ice, which is shown in the Appendix. The shape of the main peak also seems to have an asymmetric profile that is skewed in the opposite sense to that arising from the defective cubic ice formation. Since the DSC measurements show a double transition, it seems probable that lda-ice is present at the interfacial layer and is more easily created for the non-modified sample, as indicated by the different shapes shown in Figure 13. This view is supported by the complete absence of higher order Bragg peaks that are clearly seen in Figure 11 for the f=0.45 case. Consequently, there seems to be a clear signature for a direct conversion of under-cooled water to

an amorphous ice form. A more recent study with a higher Q-resolution has confirmed this conjecture.

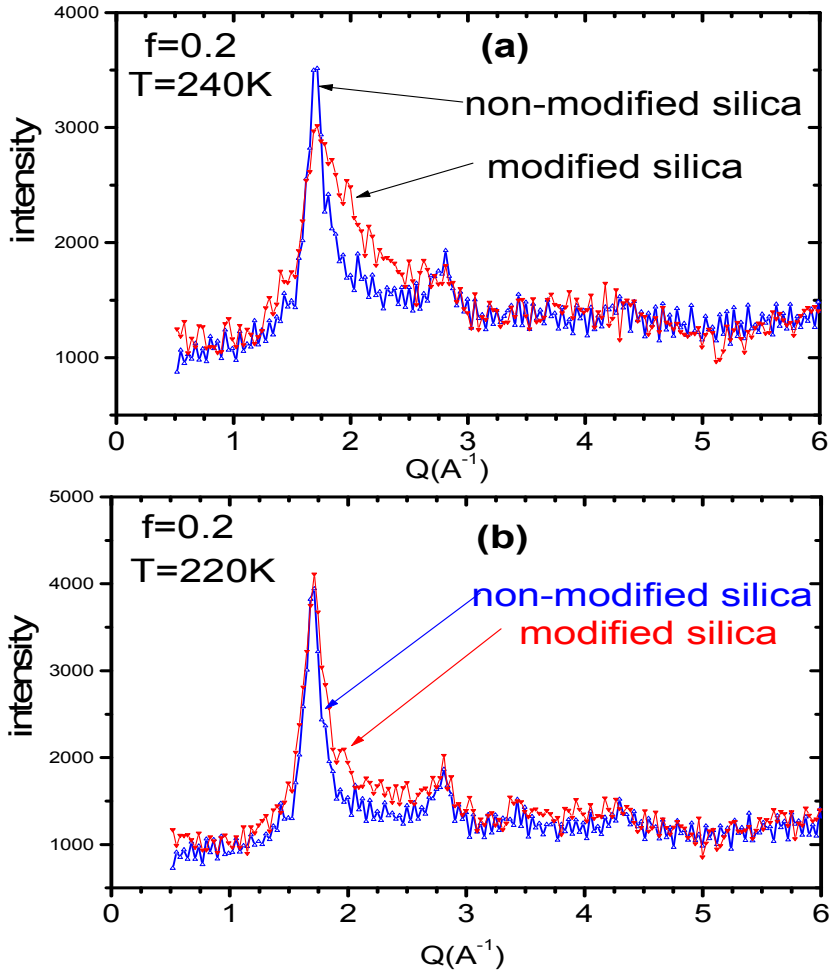

Figure 13: A comparison of the diffraction patterns for f=0.2 for the two samples at a) 240K and b) 220K.

4.3 Composite ice structure

The neutron diffraction data indicate that the ice formed inside the pores is a complex mixture of crystalline phases with characteristics of hexagonal and cubic ice, with a diffuse scattering component that could result from a defective crystalline state but is more likely to be due to the presence of a separate disordered state that relates to an amorphous network structure. The relative proportions of these independent phases are strongly temperature-dependent

and the structural features seem to show reversibility on the cooling and heating cycles. NMR relaxation studies[7,26] on ice in several different forms of silica have shown that the proton mobility is intermediate between that of bulk water and that of brittle ice. Both these NMR relaxation studies and prior NMR pulsed field gradient (PFG) studies in similar systems[32,33] suggest that this motion is predominantly rotational rather than translational. As the temperature is reduced, the relaxation process changes gradually without any obvious discontinuities once the initial nucleation has occurred. The faster dynamics are believed to be primarily due to changes in the rotational freedom arising from the creation of a more hydrogen-bonded local environment. The term, 'plastic crystal' has been used to describe this state, in analogy with other crystals that have well-defined lattice structures with disorder imposed through the variation of angular correlations. The diffraction pattern for these rotationally-disordered structures has a number of strong Bragg peaks at low and intermediate Q-values but they become rapidly attenuated at higher Q-values due to a large effective Debye-Waller factor; a typical example is cyclohexane[34]. These features are most clearly seen above 6 Å^{-1}, where all the Bragg peaks disappear to leave an oscillatory pattern that resembles the molecular form-factor of the isolated water molecule

The properties of the ice also seem to depend on the filling-factor. Hexagonal ice is only created when the pores are fairly full and during the initial stages of nucleation. Furthermore, it seems that it originates in the centre of the pore where the water characteristics are least influenced by the proximity to the interface. This process presumably arises when a small proto-crystallite begins to increase in size and there is some uncertainty in the establishment of definitive lattice directions for growth. Under these circumstances, it would seem that there will be many stacking faults in the crystal as a regular 'abcabc' or 'ababab' sequence would not have become established until a larger size had been achieved. It is noticeable that studies of cubic ice in the bulk phase[35] never seem to give a single central peak as predicted from the ideal structure factor. They also show that the various models of the defects lead to broadened peaks that can be well fitted to the experimental measurements. However, the profiles do not exhibit the diffuse scattering features seen in the data for the confined ice of the present measurements so that a separate explanation is needed for the presence of this component. Similar observations have been made in higher-resolution studies with SBA-15 mesoporous silicas[24,25] where a broad peak has been extracted from the composite profile and identified as an intermediate density form of amorphous ice.

The diffraction profile for low-density amorphous ice[36] is presented in the Appendix. It is well known from other studies[1] that as the temperature is reduced for the liquid phase there are significant changes in the diffraction pattern that become progressively larger as the water is super-cooled down to 240 K. The main diffraction peak becomes displaced towards 1.7 Å^{-1}, which is also the position for the central peak of hexagonal ice and the main peaks for both cubic and lda ice. Consequently, the position of this peak in the present data does not give any discrimination of the type of ice that has been formed. The infor-

mation can only be extracted from the rest of the diffraction profile and this is obviously difficult in the present case because the peak widths are also affected by diffraction broadening arising from the distributed nature of the water/ice volume. Within a reduced sample volume, it becomes impossible to differentiate between a liquid and a glassy state. However, there are some possible indicators in the present data.

The almost universal presence of a defective cubic-ice form for studies of ice formation in confined volumes of mesoscopic dimensions implies that there is some process that inhibits the growth of a full lattice with this structure. Johari[2] and Guillot[37] have commented on the energy criteria that may favour the formation of cubic over hexagonal ice but why the cubic form is apparently so dominant for ice formation in confined geometry is still not understood.

For the low filling-factor of 0.2, a uniformly distributed water layer would be expected to have a thickness of only 7Å corresponding to several molecular layers. Under these circumstances the diffraction pattern would be expected to show significant diffraction-broadening effects due to the restricted crystal dimensions. However, the measurements at 220K shown in Figure 13b indicate that a well-defined state is created with one clear peak. It is possible that the crystallite size is larger due to extension along the pore axis or even that larger clusters of water droplets can bridge the pore diameter. In the case of the hydrophilic sample, it can be assumed that the water wets the surface, although the distribution of the water volume may be influenced by the surface density of the surface siloxyl groups. Consequently, the imposition of a regular periodicity along the interface can only be achieved by negating the influence of the randomly-distributed H-bond sites. It is interesting that the same features are also observed for the hydrophobic sample where it would be expected that the water layer would not necessarily have a connected uniform layer. It is commonly believed that there is a thin layer of water or disordered water/ice that is 'in contact' with the interface and is 'unfreezeable'. The present studies indicate that a three molecule thick layer is actually in a condition of enhanced rotational motion ("plastic ice") but can convert to brittle ice if the temperature is low enough although the temperature for the formation is different in the hydrophilic and hydrophobic surface cases.

5 Summary and futher work

It is clear from the preceding sections that the behaviour of water and ice in contact with hydrophilic and hydrophobic interfaces within a mesoporous solid is quite complex. However, the use of several different experimental techniques has provided a complementary approach that has enabled some important conclusions to be reached. In this work data from similar fillings are compared in the same silica with both modified and unmodified surfaces, and thus it is believed it is possible to elucidate the changes due to the alteration in the surface properties.

There are other ways in which water in contact with a hydrophobic interface

can be investigated. One of these is to use carbon nanotubes, as the water is readily adsorbed into the interior of the tubes. However, the pore diameters are usually much smaller and there is also the possibility of water being present on the outside of the nanotubes. However, current on-going studies[39,39] with carbon nanotubes of ∼30 Å reveal that the water properties are found to be quite distinctive and considerably different from the results obtained in this current study.

Some features are similar to those already seen in other work on templated mesoporous silicas[23,24,25,26]. However, some new results have also been obtained, particularly in relation to the use of the modified sample with a hydrophobic interface:-

- the partially-filled samples display significantly different phase transformations:-

  (a) for the 'almost full' samples with f=0.90, there is an initial formation of hexagonal ice followed by growth of cubic ice at lower temperatures,

  (b) for f=0.45, there is a single transition corresponding the formation of cubic ice - the hexagonal ice phase is not seen,

  (c) for f=0.20, there is a double transition and the diffraction peak is broadened compared with the other cases – the two samples have a different behaviour with respect to temperature and this is probably due to a difference in the distribution of the water/ice within the pore volume and at the interface.

- A molecular layer consisting of only three molecules on the internal surface of either sample, for f=0.2, appears to form a glassy state when the temperature is reduced to 240K for the non-modified case and 220K for the modified case. At lower temperatures, this state converts to a defective crystalline state.

These new results can be explained in terms of different processes that are critically dependent on the amount of water in the pore volume and the associated connectivity of the droplets. The systematic change with the pore filling-factor can be rationalised in the following terms:-

- for high filling-factors (f∼0.9), the nucleation begins at the centre of the pores and is predominantly hexagonal ice but at lower temperatures the growth phase is entirely in the form of cubic ice which increases at the expense of a disordered form of ice; in effect the central core of ice expands radially as the temperature is reduced

- for intermediate filling factors (0.4<f<0.6), there is no hexagonal ice in the core region to initiate a phase change and a lower temperature is required to create nucleation at the air-water interface; this ice does not contain any hexagonal form and subsequently grows as cubic ice

- for low coverage conditions (f∼0.2) the water layer thickness is small and corresponds to only a few molecular layers if distributed uniformly on the surface: in this case, the strong difference in the behaviour as a function of temperature for the two samples is probably related to the connectivity of the water volume, and both systems produce a disordered or glassy phase at low temperatures.

There are obviously many unanswered questions that remain and further work is continuing to try to unravel the complexities that have been observed. A second paper with additional measurements on the same samples is in preparation[40]. In addition further studies of these and other porous silicas are continuing, comparing NMR cryoporometric measurements with those by a range of other techniques including gas absorption and small angle neutron scattering[38].

Although the present study has adopted an essentially 'chemical physics' approach to these characteristics using synthetic mesoporous materials, there are many aspects of liquid behaviour and ice nucleation in confined geometry that relate to other disciplines. These topics include aspects of water structure at protein interfaces, in bio-membranes and other disciplines such as geological rock structures, glaciology and perhaps, even astro-chemistry. There are also commercial interests relating to cryo-protection, filtration and controlled delivery of chemicals.

6 Acknowledgements

One of us (JJ) wishes to acknowledge a grant from Parténariat Hubert Curien UTIQUE /18565UB-CMCU / O8G1302 that has enabled experimental work to be conducted at several different laboratories The investigation has also been undertaken as part of a thesis to be submitted to the University of Orsay, Paris, and the University of Monastir, under the supervision of M-C Bellissent-Funel. Another one of us (JBWW) acknowledges partial support from EPSRC grant EP/D052556/1: "Capillary controls on gas hydrate growth and dissociation in synthetic and natural porous media: PVT, NMR, Neutron Diffraction and SANS", with the Institute of Petroleum Engineering at the University of Heriot Watt. HC acknowledges financial support from the Netherlands Technology Foundation STW and the EOS technology programme of the Dutch Ministry of Economic Affairs.

7 Appendix

There is a wide literature on a range of amorphous ice structures prepared by different routes. Most of these ices eventually convert to the low-density form after annealing at higher temperatures in the region of 120K. The neutron diffraction pattern[36] for low-density amorphous [lda] D_2O ice is shown in Figure 14. It differs from that of ambient bulk water in several respects – i) the main peak is displaced from 1.98 $Å^{-1}$ to 1.70 $Å^{-1}$ and is sharper, ii) there is a more developed

oscillatory structure in the region of 2.5-3.5 $Å^{-1}$. The structural features are well represented by a model based on a random fourfold-co-ordinated network of tetrahedral hydrogen bonds[41]. This form is sometimes regarded as the limiting case of water at low temperatures where there is complete connectivity and the diffusional motion has effectively been 'frozen'[42]. At a temperature of 140 K, the lda-ice converts to a defective form of cubic ice that subsequently transforms to hexagonal ice at a much higher temperature. For many years it was thought impossible to create amorphous ice directly from the liquid phase but this was achieved in 1991 by Mayer and colleagues[43] using a hyper-quench technique. It is accepted that the lda-form is a well-defined amorphous state of ice although there is still considerable controversy over whether a single high-density form exists or whether there are actually many metastable states produced by different fabrication routes.

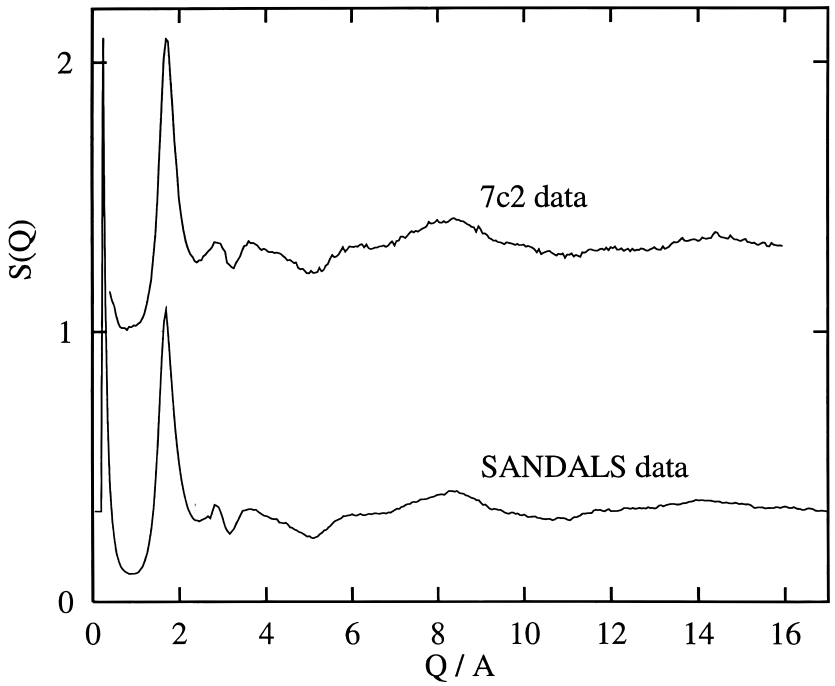

Figure 14: - A1. The structure factor S(Q) for D_2O as measured on 7C2 and SANDALS.[36]

8 Figure captions:

1. Nitrogen adsorption/desorption for non-modified and modified mesoporous silica samples.

2. DSC measurements for D_2O water in the non-modified and modified samples with filling factors, f, of 0.90, 0.45 and 0.20.

3. NMR cryoporometry measurements for H_2O water in a non-modified sample with filling factor f=1.98, a modified sample with f=1.69 and for a modified partially-filled sample with a filling factor f=0.63, for both cooling and warming ramps.

4. The pore size distribution function for both samples determined from the NMRC data of Fig 3.

5. The measured intensity profiles for neutron scattering from 'dry' and 'wet' silica samples with the cryostat background; the pattern for the water is shown below.

6. The superimposed diffraction patterns for water/ice in the

   non-modified silica sample as a function of temperature; showing the low-Q region on an expanded scale: a) cooling, b) heating.

7. The change in the low-Q intensities as a function of temperature a) non-modified silica, b) modified silica.

8. The growth of ice for f=0.9, shown as a difference function for both samples a) between 297 and 260K, and b) between 260 and 220K.

9. The growth of ice for f=0.2, shown as a difference function for both samples between 255 and 220K.

10. The diffraction pattern for the non-modified sample with f=0.2, between 220 and 200K; the difference function is shown below.

11. The diffraction patterns for f=0.45 for both samples at several temperatures.

12. The diffraction patterns for f=0.2 at various temperatures for a) non-modified and b) modified samples.

13. A comparison of the diffraction patterns for f=0.2 for the two samples, a) 240K and b) 220K.

14. A1. S(q) for D_2O as measured on 7C2 and Sandals.

9 Tables

1. The temperatures of different peaks in the DSC measurements for cooling and heating cycle

2. Pore characterisation by N_2 gaz adsorption and NMR Cryoporometry

3. Experimental variables for the neutron measurements

References

[1] J. Dore, *Chem. Phys.*, 2000, **258**, 327–347.

[2] G. P. Johari, *Journal Of Chemical Physics*, 2005, **122**, 194504.

[3] H. K. Christenson, *Journal of Physics-Condensed Matter*, 2001, **13**, R95–R133.

[4] B. Webber and J. Dore, *J. Phys.: Condens. Matter*, 2004, **16**, S5449–S5470.

[5] H. Thompson, A. K. Soper, M. A. Ricci, F. Bruni and N. T. Skipper, *Journal Of Physical Chemistry B*, 2007, **111**, 5610–5620.

[6] J. Wang, Y. W. Tang and X. C. Zeng, *Journal Of Chemical Theory And Computation*, 2007, **3**, 1494–1498.

[7] J. B. W. Webber, *Progress in NMR Spectroscopy*, 2009, **Invited, 10.1016/j.pnmrs.2009.09.001**, 1.

[8] R. Iler, *The Chemistry of Silica*, Wiley & Sons Inc., New York, USA, 1979.

[9] H. L. Castricum, M. C. Mittelmeijer-Hazeleger, A. Sah and J. E. ten Elshof, *Micropor. Mesopor. Mat.*, 2006, **88**, 63–71.

[10] S. Brunauer, P. H. Emmett and E. Teller, *J. Am. Chem. Soc.*, 1938, **60**, 309–319.

[11] S. J. Gregg and K. S. W. Sing, *Adsorption, Surface Area and Porosity*, Academic Press, London, 2nd edn., 1982, p. 42.

[12] ISO, *ISO 9277:1995. Determination of the specific surface area of solids by gas adsorption using the BET method*, 1995, `http://www.iso.org/iso/catalogue_detail.htm?csnumber=16928`.

[13] E. P. Barret, L. G. Joyner and P. P. Halenda, *J. Am. Chem. Soc.*, 1951, **73**, 373–380.

[14] A. Lecloux and J. P. Pirard, *J. Colloid Interf. Sci.*, 1979, **70**, 265–281.

[15] J. Mitchell, J. B. W. Webber and J. Strange, *Phys. Rep.*, 2008, **461**, 1–36.

[16] J. B. W. Webber, *Phd*, Physics, University of Kent at Canterbury, UK. , 2000.

[17] J. B. W. Webber, *Magn. Reson. Imaging*, 2003, **21**, 428.

[18] O. Petrov and I. Furo, *Physical Review E*, 2006, **73**, 7.

[19] J. B. W. Webber and J. C. Dore, *Nucl. Instrum. Meth. A.*, 2008, **586**, 356–366.

[20] S. Jaehnert, F. V. Chavez, G. E. Schaumann, A. Schreiber, M. Schoenhoff and G. H. Findenegg, *Phys. Chem. Chem. Phys.*, 2008, **10**, 6039–6051.

[21] J. B. W. Webber, J. H. Strange and J. C. Dore, *Mag. Res. Imag.*, 2001, **19**, 395–399.

[22] B. Beuneu, 2003, `http://www-llb.cea.fr/spectros/pdf/7c2-llb.pdf`.

[23] E. Liu, J. C. Dore, J. B. W. Webber, D. Khushalani, S. Jähnert, G. H. Findenegg and T. Hansen, *J. Phys.: Condens. Matter*, 2006, **18**, 10009–10028.

[24] J. Seyed-Yazdi, Farman, J. C. Dore, J. B. W. Webber, G. H. Findenegg and T. Hansen, *J. Phys.: Condens. Matter*, 2008, **20**, 205107, (10 pp).

[25] J. Seyed-Yazdi, H. Farman, J. C. Dore, J. B. W. Webber and G. H. Findenegg, *J. Phys.: Condens. Matter*, 2008, **20**, 205108, (12 pp).

[26] J. B. W. Webber, J. C. Dore, J. H. Strange, R. Anderson and B. Tohidi, *J. Phys.: Condens. Matter*, 2007, **19**, 415117 (12pp).

[27] G. Plazeck, *Phys. Rev.*, 1952, **86**, 377.

[28] J. G. Powles, *Adv. Phys.*, 1973, **22**, 1–56.

[29] M. C. Bellissent-Funel, L. Bosio and J. Teixeira, *J. Phys-Condens. Mat.*, 1991, **3**, 4065–4074.

[30] K. Yoshida, T. Yamaguchi, S. Kittaka, M.-C. Bellissent-Funel and P. Fouquet, *J. Chem. Phys.*, 2008, **129**, 054702.

[31] J. M. Zanotti, G. Gibrat and M. C. Bellissent-Funel, *Phys. Chem. Chem. Phys.*, 2008, **10**, 4865–4870.

[32] H. F. Booth and J. H. Strange, *Mol. Phys.*, 1998, **93**, 263–269.

[33] H. F. Booth and J. H. Strange, *Magn. Reson. Imaging*, 1998, **16**, 501–504.

[34] H. Farman, J. C. Dore and J. B. W. Webber, *J. Mol. Liq.*, 2002, **96-97**, 353–362.

[35] T. C. Hansen, M. M. Koza, P. Lindner and W. F. Kuhs, *Journal Of Physics-Condensed Matter*, 2008, **20**, 258105.

[36] D. Blakey, *PhD Thesis,*, Physics,, University of Kent at Canterbury, UK., 1994.

[37] B. Guillot and Y. Guissani, *J. Chem. Phys.*, 2003, **119**, 11740–11752.

[38] J. Webber, J. Strange and J. Dore, in preparation.

[39] J.C.Dore, T.Ohba, K.Kaneko, S.Iijima, A.Burian and A.C.Hannon, submitted.

[40] H. L. Castricum, J. Jelassi, J. C. Dore, J. B. W. Webber, M. C. Bellissent-Funel and R. Dorbez-Sridi, In Preparation.

[41] M. R. Chowdhury, J. C. Dore and J. T. Wenzel, *Journal Of Non-Crystalline Solids*, 1982, **53**, 247–265.

[42] L. Bosio, G. P. Johari, M. Oumezzine and J. Teixeira, *Chem. Phys. Lett.*, 1992, **188**, 113–118.

[43] A. Hallbrucker, E. Mayer, L. P. Omard, J. C. Dore and P. Chieux, *Phys. Lett.*, 1991, **159**, 406–410.